

Adsorptive Removal of Reactive Blue 25 and Reactive Blue 49 Dyes from Aquatic Solutions Using Zinc Oxide Nanoparticles

Zahra Monsef Khoshhesab*, Mohammadreza Mohammadi Pour Salehloo

Department of Chemistry, Payame Noor University, 19395-4697, Tehran, Iran

Received: 24 August 2021

Accepted: 22 September 2021

DOI: 10.30473/ijac.2022.62547.1220

Abstract

In this work, Zinc oxide nanoparticles (ZnONPs) were utilized as a potential adsorbent for the adsorption of Reactive Blue 25 (RB25) and Reactive Blue 49 (RB49) dyes from aqueous solutions. ZnONPs adsorbent was synthesized by precipitation method and characterized using XRD, TEM, SEM, and N₂ adsorption/desorption techniques. The effect of various parameters including solution pH, shaking time, adsorbent amount and initial concentration of the dyes on the adsorption efficiency was studied. The experimental adsorption data analyzed with various kinetic and isothermal methods. The adsorption kinetic study revealed that the adsorption process followed pseudo-second-order kinetic model. Additionally, adsorption isotherm studies indicated that adsorption equilibrium data were well fitted to Langmuir model and accordingly, the maximum adsorption capacity of the adsorbent for RB25 and RB49 found to be 34.36 and 34.60 (mg/g), respectively. From this study, ZnONPs is suggested as an effectual adsorbent for the removal of dyes from aqueous samples.

Keywords

Reactive Blue 25; ZnO Nanoparticles; Reactive Blue 49; Dye Removal ; Water Treatment.

1. INTRODUCTION

Various industries such as textile, paper, plastics, leather, food and cosmetics utilize extensive amounts of synthetic dyes which can impose serious environmental problems. The dyes discharged into water streams cause undesirable color and are known to be carcinogenic and toxic [1-3]. The colored effluents released into water stream may undergo chemical and biological changes, consuming dissolved oxygen. Also, release the dye into water interrupts aquatic communities present in ecosystem by reducing and obstructing sun light penetration [4]. In addition, most of the used dyes and their degradation products are toxic and harmful for humans [5]. Thus, the treatment of dye-contaminated wastewater has become a significant problem in nowadays [6-10]. Several methods such as coagulation/flocculation, membrane treatment, ion exchange, oxidative degradation, photo degradation, biological and photochemical degradation, anaerobic/aerobic treatment, electrochemical methods and adsorption are developed for the dye removal from wastewater [11-12]. However, adsorption technique has attracted more attention for wastewater treatment due to its high efficiency, ease of operation, and simplicity of design [13-15]. Additionally, the majority of industrial dyes are chemically and biologically stable and their degradation using the chemical and biological methods are ineffective. Therefore, adsorption can be considered as the

most efficient technique for the treatment of contaminated water. [16-20].

ZnO has many attractive properties such as high photocatalytic activity, the wide band gap (3.17 eV), non-toxicity, biocompatibility, biosafety and simple method of preparation [21]. Concerning the unique properties of nanomaterials, nano-sized ZnO has attracted more attention in optoelectronics, sensors, transducers, cosmetics ingredients, medicine drug carriers, biosensors and water treatment [22]. In particular, due to biocompatibility and biosafety, ZnO has gained an increasing interest in environmental applications. However, the majority of the investigations has been focused on the photocatalytic activity of ZnO and a few studies has been developed for its adsorptive properties [13,23]. Therefore, in this study, ZnONPs were applied as adsorbent for the removal of Reactive Blue 25 (RB25) and Reactive Blue 49 (RB49) as models of azo and anthraquinone dyes, respectively, through a batch system. These dyes are extensively utilized in textile industries for cotton and viscose dyeing. RB25 and RB49 are very toxic, mutagenic, carcinogenic and non-biodegradable. Despite the extensive application of the dyes in various industries, a few studies have been performed for their removal. Chitosan-activated sludge composites and coal based bottom ash were applied as adsorbent for the removal of RB49 from aqueous solutions [24-25]. Also, the degradation of RB 49 was investigated using activated carbon

*Corresponding Author: monsef_kh@pnu.ac.ir

in catalytic ozonation system [26]. The aim of this work was to investigate the effectiveness of ZnONPs in the removal of dyes. In this regard, the experimental variables influencing the adsorption efficiency such as initial dye concentration, solution pH, contact time and adsorbent dosage were optimized by one variable- at-a time method. The adsorption process was investigated using Langmuir and Freundlich isotherms. Also, the pseudo-first-order and pseudo-second-order models were used to evaluate the kinetic data.

2. EXPERIMENTAL

2.1. Materials and methods

Ammonium hydrogencarbonate, thiourea, sodium hydroxide and hydrochloric acid (analytical grade) were all supplied purchased by Merck Chemical Co. (Germany). ZnO powder (approximately 20 μm) was purchased from Loba Chemie Co. (India). The commercial Reactive Blue 49 ($\text{C}_{32}\text{H}_{23}\text{ClN}_7\text{Na}_3\text{O}_{11}\text{S}_3$, M.W: 882.186 g mol^{-1}) and Reactive Blue 25 ($\text{C}_{34}\text{H}_{25}\text{K}_2\text{N}_{11}\text{O}_{11}\text{S}_3$, M.W: 811.499 g mol^{-1}) was obtained from a local textile industry (Iran). The chemical structures of the dyes are shown in Fig. 1. All chemicals used as received without further purification and all aqueous solutions were prepared with double distilled water. Stock solution of the dyes (1000 mg L^{-1}) was prepared by dissolving an accurately weighed quantity of the dyes in water. The working solutions of each dye were prepared by stepwise diluting the stock solution with water. The pH of sample solution was adjusted with NaOH or HCl (0.10 mol L^{-1}) solutions.

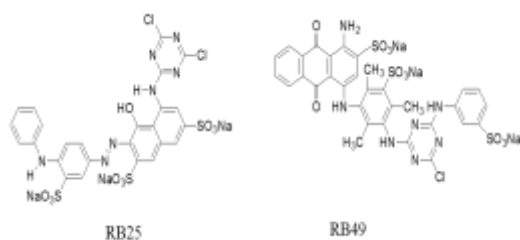


Fig. 1. Chemical structures of RB25 and RB49.

2.2. Preparation of adsorbent

The ZnONPs was prepared according the procedure described in Ref. [27]. 2.4 g of commercial ZnO powder was added into 6.0 mL NH_4HCO_3 aqueous solution (80% w/v) under vigorous stirring at 60 $^\circ\text{C}$ in two steps: firstly, 0.8 g ZnO was added to the prepared NH_4HCO_3 solution until dissolving was completed. Then, 0.16 g of ZnO and 0.2 g of $\text{CS}(\text{NH}_2)_2$ were added to the above solution and the mixture was stirred for another 2 h. Finally, the white precipitate was dried at 70 $^\circ\text{C}$ for 6 h, and calcined at 400 $^\circ\text{C}$ for 1h to prepare ZnONPs. The prepared nano-ZnO was utilized for the adsorption experiments.

2.3. Characterization methods

Characterization of the prepared ZnONPs was performed by an X-ray diffractometer (XRD: Philips; PW1800) using Cu-K α radiation ($\lambda = 0.15418$ nm, 40 kV, 30 mA) and its average crystalline size was calculated using Scherrer's formula as follows:

$$D_c = \frac{\kappa\lambda}{\beta_{1/2}\cos\theta} \quad (1)$$

where D_c is the crystalline diameter, K is the Scherrer constant (0.89), λ is the X-ray wavelength (0.15418 nm), $\beta_{1/2}$ is the full width at half maximum (FWHM) of the diffraction peak and θ is the diffraction angle of the peak. The morphology and particle size of the ZnONPs were investigated with scanning electron microscopy (SEM) using a KYKY EM3200 instrument (China) and transmission electron microscopy (TEM) by Philips EM208S model with an accelerating voltage of 100 kV. Surface area and porosity analysis were performed by nitrogen adsorption-desorption isotherms at 77.36 K with a Belsorp mini II (Japan) apparatus. Specific surface area of ZnONPs was calculated based on Brunauer-Emmett-Teller (BET) method and the pore size distribution of the adsorbent was also evaluated from the desorption branch of the isotherm plot using Barrett, Joyner and Halenda (BJH) method. A double beam UV-Vis spectrophotometer (Shimadzu, UV-1601, Japan) was used to measure the absorbance.

2.4. Batch removal experiments

Adsorption of RB25 and RB49 onto ZnONPs was studied through batch experiments. The optimal experimental conditions for adsorption capacity (or removal efficiency) were investigated using one variable- at-a time method, as follows: 25 ml of the dye solution (RB25 or RB49) was mixed with a known amount of adsorbent and the mixture was shaken at room temperature. After the desired exposure time, the suspension was filtered and the residual concentration of the dye in the filtrate was determined by UV-Vis spectrophotometer at the maximum wavelength of RB25 (660 nm) and RB49 (586 nm) with the pre-established calibration curves. The dye removal percentage (R%) and adsorption capacity (q_e) were calculated using Eqs. (2) and (3), respectively:

$$R\% = \frac{C_0 - C_t}{C_0} \times 100 \quad (2)$$

$$q_e = \frac{(C_0 - C_e) \times V}{m} \quad (3)$$

where C_0 is the initial concentration of the dye (mg L^{-1}) and C_t is the concentration of dye after time t (mg L^{-1}); q_e is the adsorption capacity (mg g^{-1}); C_e (mg L^{-1}) is the dye concentration at equilibrium time; V is the volume of the dye solution (L), and m is the amount of the nano-ZnO adsorbent (g).

The adsorption kinetics and adsorption isotherms were performed using a thermostatic bath at constant temperature ($25\text{ }^{\circ}\text{C} \pm 0.5$). The adsorption kinetics was done by mixing ZnONPs with 25 mL of RB25 solution (100 mg L^{-1}) or RB49 solution (50 mg L^{-1}) and the suspension was shaken for different times. To study the adsorption isotherm, 25 mL of RB25 ($25\text{--}400\text{ mg L}^{-1}$) or RB49 ($50\text{--}400\text{ mg L}^{-1}$) were mixed with 0.10 g and 0.09 g of ZnONPs, for 75 min and 10 min of contact time, respectively. Afterwards, the mixtures were centrifuged and the dye concentration in the filtrate was determined.

3. RESULT AND DISCUSSION

3.1. Characterization of ZnONPs

The crystalline phase of ZnONPs were characterized with XRD and results are presented in Fig. 2.

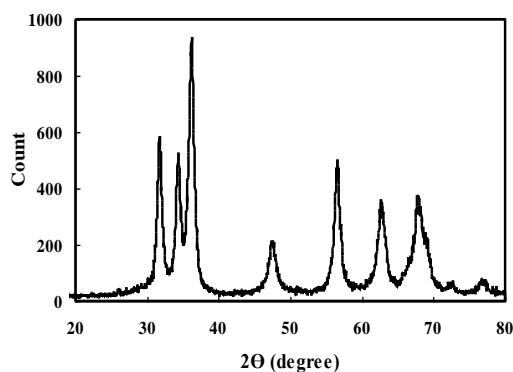


Fig. 2. The XRD pattern of ZnONPs.

The diffraction peaks appeared at 2θ of 31.8° , 34.4° , 36.3° , 47.6° , 56.6° , 62.8° , 67.9° , and 69.1° can be assigned to the ZnO hexagonal wurtzite structure (JCPDS card 36-1451), demonstrating the resultant nano-ZnO are pure. Also, based on the Scherrer's formula, Eq. (1), the average crystallite size of ZnONPs is about 12 nm. The TEM image (Fig. 3(a)) shows that ZnONPs consisted of nanoparticles with an average size of about 15 nm. The average size of ZnONPs determined by TEM is consistent with that of estimated by from XRD pattern. Fig. 3(b) shows the SEM image of ZnONPs indicating a cauliflower-like morphology. The nitrogen adsorption-desorption isotherm and the corresponding BJH pore-size distribution curve are depicted in Fig. 4, which is in accordance with a type III isotherm according to the IUPAC classification [28]. According to the BJH plot (the inset of Fig. 4), the average pore size of the adsorbent found to be about 14.1 nm. The BET surface area, the average pore diameter, and the total pore volume of ZnONPs were $23.39\text{ m}^2/\text{g}$, 33.35 nm and $0.195\text{ cm}^3/\text{g}$, respectively.

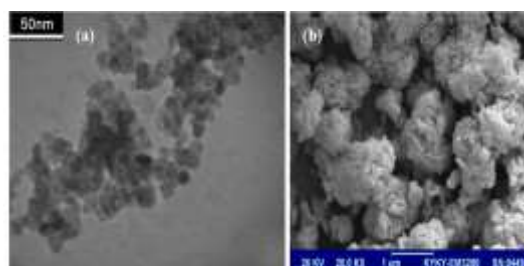


Fig. 3. The TEM (a) and SEM (b) micrograph of ZnONPs.

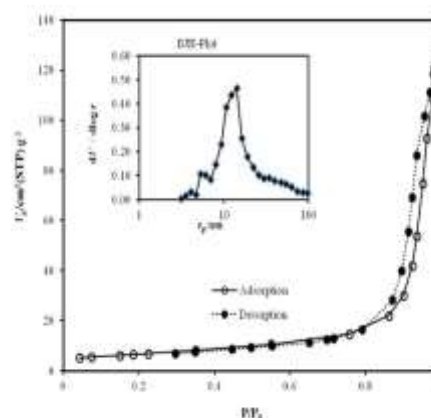


Fig. 4. N_2 adsorption/desorption isotherm curve of ZnONPs and BJH pore size distribution plot (the inset).

3.2. Optimization of adsorption conditions

The capability of ZnONPs adsorbent for the removal of textile dyes from aqueous solutions was tested using RB25 and RB49. In this regard, the experimental parameters influencing the removal efficiency (R%) such as solution pH, adsorbent amount, shaking time and initial concentrations of the dyes were studied and optimized.

3.2.1. Effect of the solution pH

To investigate the effect of the initial pH on the adsorption efficiency of RB25 and RB49 by ZnONPs, 0.05g portions of the adsorbent were contacted separately with 25 mL of RB25 (100 mg L^{-1}) and RB49 (50 mg L^{-1}) solutions at various pH values from 3 to 8 for 60 min, while the other conditions were kept constant. As it is seen from Fig. 5(a), the removal efficiency (%R) for both dyes gradually decreased with the increase in the pH and then steeply decline at pH 8. The adsorption of the anionic dyes onto ZnONPs can be assigned to ionic attractions between the surface charges of the adsorbent and anionic sulfonate ($-\text{SO}_3$) groups of the dyes. ZnO has hydroxyl groups on its surface that can be protonated depending on the pH value [29]. Since the pH of zero point charge (pH_{ZPC}) of ZnO is about 9, its surface charge becomes positive at pHs around 9 [30-31]. Therefore, the adsorption of both anionic dyes

could be mainly due to electrostatic attractions between positively charged surface of ZnO and negatively sulfonate groups of the dyes. On the other hand, at alkaline solutions, competition of OH⁻ ions with the anionic dye molecules for the positive surface of ZnO leads to decrease the removal percentage. Furthermore, the highest adsorption at higher acidic condition (pH 3) indicates that the adsorption process is predominantly controlled by electrostatic interactions between the positively charged surface of adsorbent and the anionic dye molecules.

3.2.2. Effect of shaking time

The influence of shaking time on the adsorption percentage of RB25 and RB49 was studied by mixing 0.05 g of ZnONPs with 25 mL of RB25 (100 mg L⁻¹) and RB49 (50 mg L⁻¹) followed by shaking for different periods of contact time. The removal percentage of the dyes onto the ZnONPs as a function of shaking time is illustrated in Fig. 5(b). Obviously, both dyes exhibited a similar trend for adsorption onto the ZnONPs. As shown in Fig. 5(b), removal percentage of RB49 rapidly rose from 53% to 73% within contact time of 3-10 min and then it remained constant indicating that the contact time of 10 min is sufficient to establish an equilibrium adsorption. As for RB25, the adsorption percentage of RB25 gradually increased and an equilibrium was achieved after 75 min of shaking time. Therefore, the optimal shaking time for the adsorption of RB49 and RB25 onto ZnONPs was found to be 10 min and 75 min, respectively. It is worthwhile to note that the equilibrium times for the adsorption of RB49 onto present adsorbent are remarkably shorter than the reported values for many other adsorbents [24-25].

3.2.3. Effect of adsorbent dose

The influence of adsorbent dose on the removal percentage of RB25 and RB49 was studied using different amounts of the adsorbent with 25 mL of RB25 (100 mg L⁻¹) or RB49(50 mg L⁻¹) solutions at the respective optimal pH for 15 min of contact time, respectively. As it is obvious (Fig. 5(c)), the adsorption of both dyes increased with the increase in the adsorbent dose and reached the maximum value with 0.1 g of ZnONPs for RB25 and 0.09 g for RB49. Further increasing in the adsorbent amount had no significant effect on the adsorption efficiency. Thus, 0.1g and 0.09 g of ZnONPs was found to be sufficient for the removal of RB25 and RB49 respectively. The increase in the dye removal percentage with the adsorbent dose is attributed to the rise in the number of adsorption sites.

3.2.4. Effect of initial concentration of the dyes

The effect of dye concentration on the adsorption process was investigated at 25 °C, under optimal

experimental conditions. Adsorption experiment of RB25 carried out at pH 3 with 0.1g of ZnONPs for 75 min of contact time. Adsorption of RB49 was performed with 0.09 g of ZnONPs for 10 min at pH 3. The variation of adsorption removal as a function of the dye concentration was demonstrated in Fig 5(d).

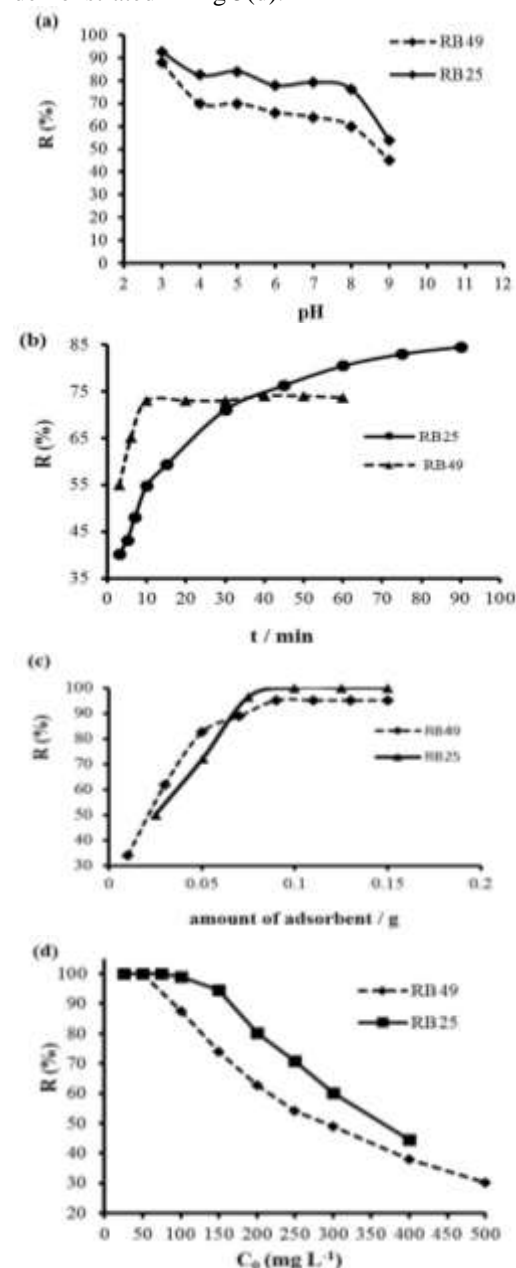


Fig. 5. Effect of various parameters on the removal efficiency of RB25 and RB49 by ZnONPs, (a) effect of pH, (b) effect of contact time, (c) effect of adsorbent amount, (d) effect of the initial dye concentration.

As expected, the percentage removal of both dyes decreased with their concentration which can be attributed to the fact that the given adsorbent dosage has limited adsorption sites. Hence, at lower concentrations, the number of dye molecules which are available in the solution is less as

compared to the available sites on the adsorbent, and at higher dye concentrations, the available sites for adsorption become fewer leading to saturate the adsorption sites. Thus, the percentage removal of the dyes decreased with the increase in their initial concentration.

3.3. Study of adsorption kinetics

Two conventional pseudo-first order and pseudo-second order kinetic models have been used to verify the adsorption mechanism and potential rate controlling steps [32-33]. The pseudo-first-order (Eq. (4)) and pseudo-second order kinetic (Eq. (5)) equations can be written in the following forms:

$$\ln(q_e - q_t) = \ln q_e - k_1 t \quad (4)$$

$$\frac{t}{q_t} = \frac{1}{k_2 q_e^2} + \frac{t}{q_e} \quad (5)$$

where k_1 (min^{-1}) and k_2 ($\text{g mg}^{-1} \text{min}^{-1}$) are the pseudo-first order and pseudo-second order rate constants, q_e and q_t (mg g^{-1}) are the amounts of dye adsorbed at equilibrium and at time t (min), respectively. Analysis of the experimental data using the pseudo-first order and pseudo-second order kinetic models are depicted in Fig. 6.

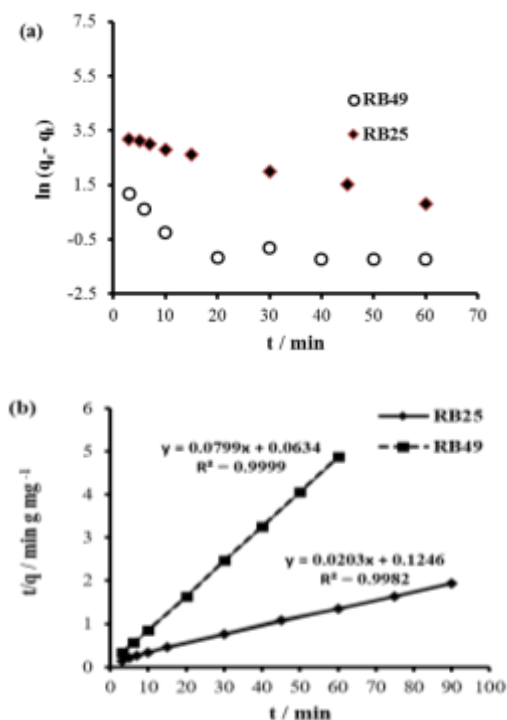


Fig. 6. Pseudo-first order (a) and pseudo-second order (b) kinetic plots of RB25 and RB49.

As it is seen from Fig. 6, for both dyes, the experimental data fitted to the pseudo-second order kinetics very well (Fig. 6(b)) while their agreement with the pseudo-first order model was

very poor (Fig. 6(a)). Thus, only the kinetic parameters derived from the pseudo-second order plots are presented in Table 1. The high R^2 values (0.9999, 0.9982) besides the good agreement between the experimental q_e ($q_{e,\text{exp}}$) and the calculated q_e ($q_{e,\text{cal}}$) using Eq. (5) indicate that the adsorption of RB25 and RB49 onto ZnONPs can be well described by the pseudo-second order model suggesting a chemisorption process [5, 34, 35].

Table 1. Pseudo-second order kinetic parameters of RB25 and RB49 onto ZnONPs at 25 °C.

Type of dye	$q_{(\text{exp})}$ (mg g^{-1})	$k_2 / \text{g mg}^{-1} \text{min}^{-1}$	$q_e (\text{cal}) / \text{mg g}^{-1}$	R^2
RB25	46.50 ± 1.15	0.0033 ± 0.0062	49.26 ± 0.27	0.9982
	12.30 ± 0.56	0.1007 ± 0.0090	12.51 ± 0.09	0.9999

3.4. Adsorption isotherm

An adsorption isotherm describes the relationship between the amount of the adsorbed species per unit mass of adsorbent (q_e , mg/g) and the non-adsorbed amount of the target in bulk solution (C_e , mg/L) at a given temperature. Adsorption isotherm study is very important tool to describe the adsorption process because it provides useful information about adsorption mechanisms, surface properties and adsorption capacity of an adsorbent towards an adsorbate [1, 5, 36]. In this research, Langmuir and Freundlich isotherm models have been used for analyzing of the equilibrium adsorption data [36, 37]. The Langmuir model is based on the monolayer adsorption of the target molecules on a uniform surface with a finite number of adsorption sites. This model assumes that the adsorption takes place on a homogenous surface without any interactions between adsorbate molecules. The Freundlich isotherm is an empirical equation based on the multilayer adsorption of the target molecules on a heterogeneous surface which adsorption capacity is related to the concentration of adsorbate. The linear form of Langmuir (Eq. (6)) and Freundlich (Eq. (7)) isotherms can be presented as the following equations:

$$\frac{C_e}{q_e} = \frac{1}{K_L q_m} + \frac{C_e}{q_m} \quad (6)$$

$$\ln q_e = \frac{1}{n} \ln C_e + \ln K_f \quad (7)$$

where q_e is the amount of adsorbed per unit mass of adsorbent (mg g^{-1}), C_e is the equilibrium

concentration of the adsorbate (mg L^{-1}), q_m is the monolayer adsorption capacity (mg g^{-1}), K_L is Langmuir adsorption constant related to the affinity of binding sites (L mg^{-1}) of adsorbent toward the adsorbate. K_f ($\text{mg/g (L/mg)}^{1/n}$) is Freundlich constant which refers to the adsorption capacity, and n is the heterogeneity factor related to the adsorption intensity, indicating the favorability of adsorption. The Langmuir constants are calculated from the slope and intercept of plot of C_e/q_e versus C_e and the parameters of Freundlich isotherm are calculated from the slope and intercept of plot of $\ln q_e$ versus $\ln C_e$. Further, the favorability of the dye adsorption on the ZnONPs was evaluated using the dimensionless constant, R_L , called the separation factor [37], according to the following equation:

$$R_L = \frac{1}{1 + k_L C_0} \quad (8)$$

where K_L (L mg^{-1}) signifies Langmuir constant and C_0 is the highest initial dye concentration in solution (mg L^{-1}). The value of R_L indicates the adsorption process is unfavorable ($R_L > 1$), linear ($R_L = 1$), favorable ($0 < R_L < 1$), or irreversible ($R_L = 0$). The adsorption isotherms of RB25 and RB49 by ZnONPs were performed under the optimal experimental conditions at 25°C and the results are illustrated in Fig. 7(a) and 7(b). It is seen that the adsorption capacity of both dyes rose steeply and then was maintained constant corresponding to the maximum adsorption capacity. The adsorption isotherms of RB25 and RB49 on ZnONPs are regressively analyzed with Langmuir and Freundlich models and the fitted plots are presented in Fig 7 (the insets) and 8, respectively. The parameters obtained from two models are summarized in Table 2. From the R^2 values of the Langmuir and Freundlich models (Table 2) and fitting curves shown in Fig. 7 (the inset) and 8, adsorption of both dyes on ZnONPs is concluded to be in accordance with Langmuir isotherm, suggesting monolayer adsorption of RB25 and RB49 onto ZnONPs surface. Based on the Langmuir model, maximum adsorption capacities (q_m) of RB25 and RB49 on ZnONPs found to be 34.36 mg g^{-1} and 34.60 mg g^{-1} , respectively. These results are in good accordance with the q_e values observed from equilibrium isotherm (see Fig. 7(a) and (b)), when the adsorption capacities reached the maximum values and equilibrium was established.

The calculated values of R_L for adsorption RB25 and RB49 found to be 0.0017 and 0.0211 respectively, indicating the favorability of

adsorption process of these dyes onto ZnONPs adsorbent.

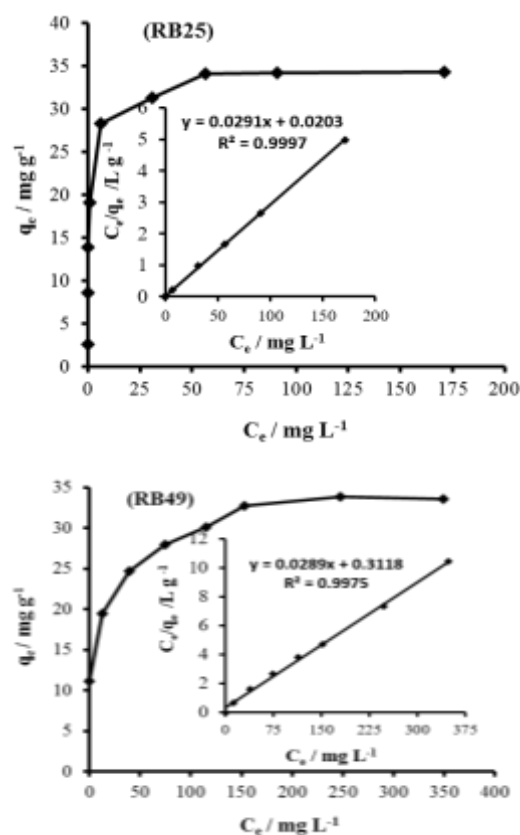


Fig. 7. Adsorption isotherms of RB25 and RB49 (at pH 3) on ZnONPs at 25°C . The insets: the linear dependence of C_e/q_e on C_e based on the Langmuir isotherm model. (for RB25: adsorbent dose, 0.10 g ; Shaking time, 75 min, and for RB49 : adsorbent dose, 0.09 g ; Shaking time ,10 min).

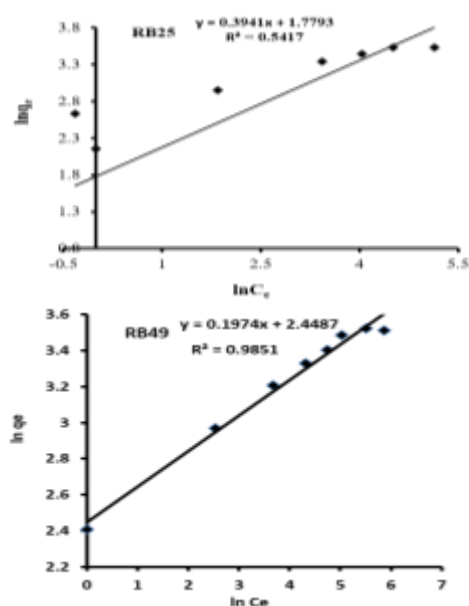


Fig. 8. The Freundlich adsorption isotherms of RB25 and RB49 on ZnONPs at 25°C (under the same conditions as Fig. 7).

Table 2. The parameters of adsorption isotherm of RB25 and RB49 onto ZnONPs at 25 °C.

Isotherm model	Parameters	RB25	RB49
Langmuir	q_m (mg g ⁻¹)	34.36 ± 0.68	34.60 ± 0.92
	K_L (L mg ⁻¹)	1.4335 ± 0.0700	0.0927 ± 0.0901
	R_L	0.0017 ± 0.0054	0.0211 ± 0.0018
	R^2	0.9997	0.9975
Freundlich	K_F (mg/g (L/mg) ^{1/n})	4.93 ± 1.61	11.57 ± 1.54
	n	2.28 ± 0.80	5.06 ± 0.59
	R^2	0.5973	0.9851

4. CONCLUSION

The applicability of ZnONPs as an adsorbent was investigated for the removal of RB25 and RB49 as models of azo and anthraquinone dyes from aqueous solutions. The experimental parameters influencing the removal percentage of the dyes were investigated via batch experiments. The kinetic data revealed that adsorption of RB49 onto ZnONPs is fast and an equilibrium adsorption is established after 15 min, however, for RB25 an equilibrium time of 75 min was obtained. Further, the dyes can be effectively removed in a wide range of pHs, within 3-8. Based on the kinetic data, the adsorption mechanism of both dyes onto ZnONPs can be described with pseudo-second-order kinetic model. Furthermore, investigation of adsorption isotherms revealed that experimental data fit well in Langmuir model, suggesting the monolayer adsorption of the dyes on the homogenous surface of ZnONPs. Accordingly, the maximum adsorption capacities for RB25 and RB49 were found 34.36 and 34.60 mg g⁻¹, respectively. Conclusively, the good adsorptive performance provided under easy conditions besides the attractive properties of ZnONPs (like biosafety, biocompatibility, simple preparation) make ZnONPs as a suitable adsorbent for efficient removal of the dyes from dyeing effluents and contaminated water.

ACKNOWLEDGEMENTS

The authors gratefully acknowledge the financial and technical support provided by the Payame Noor University.

REFERENCES

- [1] M. El-khomri, N. El-messaoudi, S. Bentahar, A. Dbik and A. Lacherai, Removal of Cationic Dye from Aqueous Solution using Agricultural Wastes: Argan and Almond Shells, *Iran. J. Energ. Environ.* 9(4) (2018) 255- 262.
- [2] S. Sivalingam, S. Sen Efficient removal of textile dye using nanosized fly ash derived zeolite-x: Kinetics and process optimization study, *J. Taiwan Inst. Chem. Eng.* 96 (2019) 305-314.
- [3] T. Huang, M. Yan, K. He, Z. Huang, G. Zeng, A. Chen, M. Peng, L. Yuan and G. Chen, Efficient removal of methylene blue from aqueous solutions using magnetic graphene oxide modified zeolite, *J. Colloid Interface Sci.* 543 (2019) 43-51.
- [4] J. Abdi, N.M. Mahmoodi, M. Vossoughi and I. Alemzadeh, Synthesis of magnetic metalorganic framework nanocomposite (ZIF-8@SiO₂@MnFe₂O₄) as a novel adsorbent for selective dye removal from multicomponent systems, *Microporous Mesoporous Mater.* 273 (2019) 177–188.
- [5] H. Wang, H. Gao, M. Chen, X. Xu, X. Wang, C. Pan and J. Gao, Microwave-assisted synthesis of reduced graphene oxide/titania nanocomposites as an adsorbent for methylene blue adsorption, *Appl. Surf. Sci.* 360 (2016) 840–848.
- [6] EL Khomri, EL. Lacherai, and N. Messaoudi, Retention of Methylene Blue on an Agro-Source Material. International, *J. Eng. Res. Tech.* 3 (2014)1657–1662.
- [7] S. Agrawal, D. Tipre, B. Patel and S. Dave, Optimization of triazo Acid Black 210 dye degradation by *Providencia* sp. SRS82 and elucidation of degradation pathway, *Process Biochem.* 49 (2014) 110-119.
- [8] R. Pandimurugan and S. Thambidurai, Synthesis of seaweed-ZnO-PANI hybrid composite for adsorption of methylene blue dye, *J. Environ. Chem. Eng.* 4 (2016) 1332–1347.
- [9] F. A. Pavan, E. S. Camacho, E. C. Lima, G. L. Dotto, V. T. Branco and S. L. Dias, Formosa papaya seed powder (FPSP): preparation, characterization and application as an alternative adsorbent for the removal of crystal violet from aqueous phase, *J. Environ. Chem. Eng.* 2 (2014) 230-238.
- [10] J. Li, D.H.L.Ngb, P. Songa, C.K. Konga and Y. Song, Synthesis of SnO₂-activated carbon fiber hybrid catalyst for the removal of methyl violet from water, *Mater. Sci. Eng. B*, 194 (2015) 1-8.
- [11] M. Siddique, R. Farooq and A. Shaheen, Removal of Reactive Blue 19 from

- Wastewaters by Physicochemical and Biological Processes- A Review, *J. Chem. Soc. Pak.* 33 (2011) 284-293.
- [12] M. Rafatullah, O. Sulaiman, R. Hashim and A. Ahmad, Adsorption of methylene blue on low-cost adsorbents: A review, *J. Hazard. Mater.* 177 (2010) 70 - 80.
- [13] Z. Monsef Khoshhesab, K. Gonbadi and Gh. Rezaei Behbehani, Removal of reactive black 8 dye from aqueous solutions using zinc oxide nanoparticles: investigation of adsorption parameters, *Desalin. Water Treat.* 56 (2015) 1558-1565.
- [14] M. Isanejad, M. Arzani, H.R. Mahdavi and T. Mohammadi, Novel amine modification of ZIF-8 for improving simultaneous removal of cationic dyes from aqueous solutions using supported liquid membrane, *J. Mol. Liq.* 225 (2017) 800-809.
- [15] Z. Ayazi, Z. Monsef Khoshhesab, F. F. Azhar and Z. Mohajeri, modeling and Optimization of Adsorption Removal of Reactive Orange 13 on the Alginate-Montmorillonite-Polyaniline Nanocomposite via Response Surface Methodology, *J. Chin. Chem. Soc.* 64 (2017) 627-639.
- [16] K. Balasubramani, N. Sivarajasekar and M. Naushad, Effective adsorption of antidiabetic pharmaceutical (metformin) from aqueous medium using graphene oxide nanoparticles: equilibrium and statistical modelling, *J. Mol. Liq.* 301 (2020) 112-426.
- [17] Z. Monsef khoshhesab and M. Ahmadi, Removal of reactive blue 19 from aqueous solutions using NiO nanoparticles: equilibrium and kinetic studies, *Desalin. Water Treat.* 57 (2016) 20037-20048.
- [18] Y. Sun, M. Chen, H. Liu, Y. Zhu, D. Wang and M. Yan, Adsorptive removal of dye and antibiotic from water with functionalized zirconium-based metal organic framework and graphene oxide composite nanomaterial UiO-66-(OH)₂/GO, *Appl. Surf. Sci.* 525 (2020)146614-146621.
- [19] L.R. Bonetto, F. Ferrarini, C. de Marco, J.S. Crespo, R. Guégan and M. Giovanela, Removal of methyl violet 2B dye from aqueous solution using a magnetic composite as an adsorbent, *J. Water Process Eng.* 6 (2015)11-20.
- [20] A.A. Narvekar, J.B. Fernandes and S.G. Tilve, Adsorption behavior of methylene blue on glycerol -based carbon materials, *J. Environ. Chem. Eng.* 6 (2018)1714-1725.
- [21] Z. Li, R. Yang, M. Yu, F. Bai, C. Li and Z.L. Wang, Cellular Level Biocompatibility and Biosafety of ZnO Nanowires, *J. Phys. Chem. C*, 112 (2008), 20115-20117.
- [22] R. Gopikrishnan, K. Zhang, P. Ravichandran, S. Baluchamy, V. Ramesh, S. Biradar, P. Ramesh, J. Pradhan, J. Hall, A.K. Pradhan and G.T. Ramesh, Synthesis, characterization and biocompatibility studies of zinc oxide (ZnO) nanorods for biomedical application, *Nano-Micro Lett.* 2 (2010) 31-36.
- [23] Z. Monsef Khoshhesab and S. Souhani, Adsorptive removal of reactive dyes from aqueous solutions using zinc oxide nanoparticles, *J. Chin. Chem. Soc.* 52(2018)1482-1490.
- [24] D. A. Sahbaz, S. Dandil and C. Acigoz, Studies on the Removal of Reactive Blue 49 Dye from Aqueous Solution onto Chitosan-Activated Sludge Composite Particles, *Bio. Chem. Res.* 6 (2019) 19-29.
- [25] C. Jarusiripot, Removal of Reactive Dye by Adsorption over Chemical Pretreatment Coal Based Bottom Ash, *Procedia Chem.* 9 (2014) 121- 130.
- [26] S. Sangjan, M. Sratongin, A. Kawpakpor, P. Ampha, L. Jamtanom and K. Kaewbang, Activated Carbon as Heterogeneous Catalyst of Catalytic Ozonation Activity for Improvement RB 49 Dye Degradation, *Mater. Sci. Forum* 860 (2016) 105-110.
- [27] Z. Monsef Khoshhesab, M. Sarfaraz and M. AsadiAsadabad, Preparation of ZnO nanostructures by chemical precipitation method, *Synth. React. Inorg. Met.-Org. Nano-Met. Chem.* 41 (2011) 814 -819.
- [28] Y. Qin, M. Long, B. Tan and B. Zhou, RhB adsorption performance of magnetic adsorbent Fe₃O₄/RGO composite and its regeneration through A fenton-like reaction, *Nano-Micro Lett.* 6 (2014)125- 135.
- [29] H. Noei , H. Qui, Y. Wang, E. Löffler and C. Woll, The identification of hydroxyl groups on ZnO nanoparticles by infrared spectroscopy, *Phys. Chem. Chem. Phys.* 10 (2008) 7092 -7097.
- [30] G.A. Park, The Isoelectric points of solid oxides, solid hydroxides, and aqueous hydroxo complex systems, *Chem. Rev.* 65 (1965) 177-198.
- [31] N. Daneshvar, N.S. Aber, M.S. Seyed Dorraji, A.R. Khataee and M.H. Rasoulifard, Photocatalytic degradation of the insecticide diazinon in the presence of prepared nanocrystalline ZnO powders under irradiation of UV-C light, *Sep. Pur. Technol.* 58 (2007) 91-98.
- [32] Y.-S. Ho and G. McKay, Pseudo-second order model for sorption processes, *Process Biochem.* 34 (1999) 451-465.
- [33] S. Lagergren, About the theory of so-called adsorption of soluble substances. K. Sven, *Veten, Hand, Handlingar*, 24 (1898) 1-39.

- [34] V. Vadivelan, K.V. Kumar, Equilibrium, kinetics, mechanism, and process design for the sorption of methylene blue onto rice husk, *J. Colloid Interface Sci.* 286 (2005) 90-100.
- [35] K.C. Lai, L.Y. Lee, B.Y.Z. Hiew, T.C.-K Yang, G.-T. Pan, S. Thangalazhy-Gopakumar, S. Gan, Utilisation of eco-friendly and low-cost 3D graphene-based composite for treatment of aqueous Reactive Black 5 dye: Characterisation, adsorption mechanism and recyclability studies, *J. Taiwan Inst. Chem. Eng.* 114 (2020) 57–66.
- [36] I. Langmuir, I. The adsorption of gases on plane surfaces of glass, mica and platinum, *J. Am. Chem. Soc.* 40 (1918) 1361-1403.
- [37] H. Freundlich, Over the adsorption in solution, *J. Phys. Chem.* 57 (1906) 385- 471.
- [38] R. Hall, L.C. Eagleton, A. Acrivos and T. Vermeulen, Pore and solid diffusion kinetics in fixed-bed adsorption under constant pattern conditions, *Ind. Eng. Chem. Fundam.* 5 (1996) 212–223.

حذف رنگ های راکتیو آبی ۲۵ و راکتیو آبی ۴۹ از محلول های آبی با استفاده از نانوذرات روی اکسید

زهرا منصف خوشحساب*، محمدرضا محمدی پور صالح لو

گروه شیمی، دانشکده علوم، دانشگاه پیام نور، تهران، ایران

تاریخ دریافت: ۲ شهریور ۱۴۰۰ تاریخ پذیرش: ۳۱ شهریور ۱۴۰۰

چکیده

در این کار، نانوذرات روی اکسید به عنوان جاذب برای جذب رنگ های ری اکتیو آبی ۲۵ و ری اکتیو آبی ۴۹ از محلول های آبی مورد استفاده قرار گرفت. نانو ذرات روی اکسید با روش رسوبی سنتز و با استفاده از فنون SEM، TEM، XRD و جذب و واجذبی نیترژن مشخصه یابی شدند. اثر عوامل مختلف مانند pH محلول، زمان شیکر، مقدار جاذب و غلظت اولیه رنگ بر کارایی جذب مورد بررسی قرار گرفت. داده های تجربی با مدل های سینتیکی و همدماهای جذبی مختلف ارزیابی شدند. نتایج بدست آمده تبعیت سینتیک جذب از مدل سینتیکی شبه مرتبه دوم را نشان داد. همچنین، مطالعه همدماهای جذب حاکی از انطباق داده های جذبی با همدمای لانگ مویر است و بر این اساس، بیشترین ظرفیت جذب برای رنگ رای کتیو آبی ۲۵ و ری اکتیو آبی ۴۹ بترتیب ۳۴،۳۶ و ۳۴،۶۰ تعیین شد. با توجه به نتایج این تحقیق، نانوذرات روی اکسید به عنوان یک جاذب موثر و کارآمد برای حذف رنگ ها از نمونه های آبی پیشنهاد شدند.

واژه های کلیدی

ری اکتیو آبی ۴۹؛ ری اکتیو آبی ۲۵؛ نانوذرات روی؛ حذف رنگ؛ تصفیه آب.